

ISTITUTO NAZIONALE DI FISICA NUCLEARE
Laboratori Nazionali di Frascati

LNF-84/11

L.Allocca, M.Iannuzzi and A.La Monaca:
AN X-RAY DIFFRACTOMETER FOR SYNCHROTRON RADIATION

Estratto da:
Nuclear Instr. and Meth. 219, 227 (1984)

AN X-RAY DIFFRACTOMETER FOR SYNCHROTRON RADIATION

L. ALLOCCA *, M. IANNUZZI ** and A. LA MONACA

PULS (CNR-INFN), Laboratori Nazionali di Frascati dell'INFN, Frascati, Italy

Received 9 February 1983 and in revised form 6 July 1983

An X-ray diffractometer for small-angle scattering and diffraction experiments using synchrotron radiation is described. The diffractometer is in operation at the Adone storage ring at Frascati. The optical collimation is 8×10^{-5} rad. A three-dimensional goniometer carries either a two-dimensional position-sensitive drift chamber detector or a one-dimensional cylindrical drift chamber. The detectors can move along a spherical surface with radius 500 mm within an arc of 0.35 rad. The best angular resolution of the diffractometer, determined by the best resolution of the detector, is 2×10^{-4} rad.

1. Introduction

In these last years, there has been a novel interest in X-ray small-angle scattering and diffraction experi-

ments mostly motivated by an increasingly popular use of synchrotron radiation and by the performance improvement of position-sensitive detectors.

In this paper an X-ray diffractometer is described which has been built in our laboratory and is in operation at the synchrotron radiation facility of the Adone storage ring. The diffractometer has been designed

* Istituto di Fisica, University of Naples, Naples, Italy.

** Physics Department, 2nd University of Rome, Rome, Italy.

Table 1: Experimental parameters of the diffractometer.

Primary beam angular divergence (2α)	8×10^{-5} rad
Angular resolution in the plane of the detector	2×10^{-4} rad
<i>x</i> -direction	8×10^{-4} rad
<i>y</i> -direction	8×10^{-4} rad
Maximum angle covered by the beam-stopper	2×10^{-3} rad
Angle covered by residual parasitic scattering (2β)	2.4×10^{-3} rad
Total angle subtended by the drift chamber	3.5×10^{-2} rad
Total angle covered by the goniometer	0.35 rad
Minimum momentum transferred (K_{\min}) at $\lambda = 3.1 \text{ \AA}$	$8 \times 10^{-3} \text{ \AA}^{-1}$
Momentum resolution in the scattered beam, ΔK , at $\lambda = 3.1 \text{ \AA}$	$8 \times 10^{-4} \text{ \AA}^{-1}$
Apparent source brightness at the collimator entrance, at $\lambda = 2 \text{ \AA}$ (n') ^{a)}	$9.2 \times 10^{10} \text{ phot s}^{-1} \text{ mm}^{-2} \text{ mrad}^{-2}$ ($\Delta E/E = 10^{-4}$)
Cross section of the collimated primary beam	0.23 mm ²
Power incident on specimen at $\lambda = 2 \text{ \AA}$, with $\Delta\lambda/\lambda = 10^{-4}$	10^6 phot/s
Quantum efficiency of the detector ($\lambda = 2 \text{ \AA}$)	50%
<i>N</i> , number of data points simultaneously detectable in the detector	
one-dimensional operation	170
two-dimensional operation	$42 \times 170 = 7140$
<i>N'</i> , number of data points simultaneously recorded on the multichannel-analyzer	
one-dimensional operation	1×512
two-dimensional	$2(1 \times 256)$
	64×64 or $4(32 \times 32)$
	32×128 or $2(32 \times 64)$
	16×256 or $2(16 \times 128)$
	= 4096
Maximum counting capability of detector	$5 \times 10^5 \text{ cps}$
Maximum recording rate of data on multichannel-analyzer	$1.5 \times 10^5 \text{ cps}$

^{a)} The effects of Be-window absorption and monochromatic efficiency are not included.

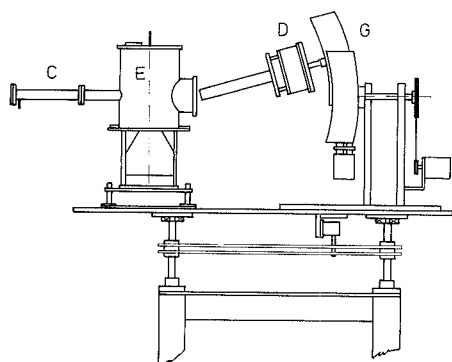


Fig. 1. General view of the diffractometer: C = collimator; E = experimental chamber; D = detector; G = goniometer.

specifically for small-angle scattering and diffraction experiments using synchrotron radiation, and presents three particular features: a) the optical collimation is very good, 8×10^{-5} rad; b) the X-ray position-sensitive detector is an electronic detector with high efficiency and high counting capability. Two types of detectors of this type are usually in operation with the diffractometer: one for two-dimensional position measurements, and the other one for one-dimensional measurements of isotropic scattering from solid or liquid disordered systems; c) a goniometer with three-dimensional movement carries the detector, and can be used both for small-angle scattering and diffraction experiments. It can be moved along a spherical surface within an arc of 0.35 rad, with a mechanical precision of $5 \mu\text{m}$.

Fig. 1 gives a general view of the diffractometer. Table 1 gives its experimental features. Fig. 2 shows the basic operational scheme of the diffractometer, which is similar to the scheme of a standard diffractometer [1]. Specific features of our design are in the construction of the collimator, the goniometer and the detector. Fig. 3 is a photograph of the apparatus.

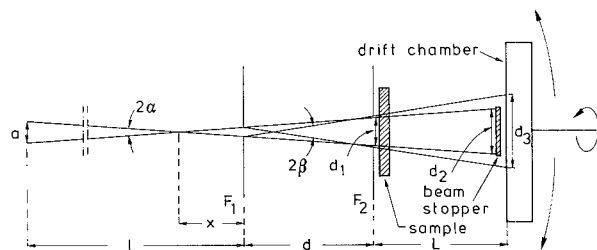


Fig. 2. Basic operational scheme of the diffractometer: a = linear size of the radiation source (ADONE); x = distance of the virtual image of the radiation source from F_1 ; l = distance source- F_1 ; L = distance F_2 -detector.

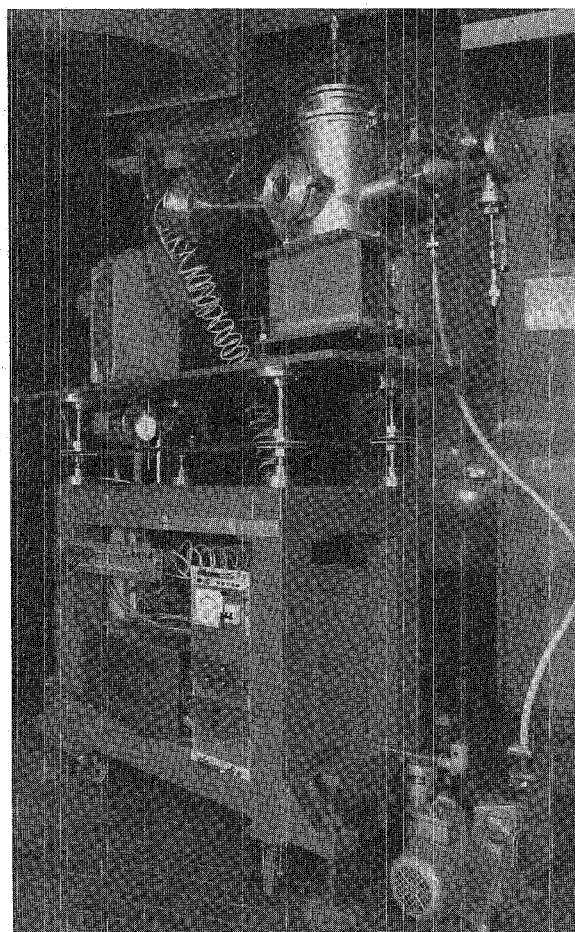


Fig. 3. Photograph of the apparatus.

2. Collimator

The collimator is basically formed by a circular pin-hole F_1 with diameter $\varnothing = 0.5$ mm located close to the exit of the X-ray monochromator, which is at a distance of 18 m from the source of synchrotron radiation (fig. 2). We point out that the intrinsic collimation and the very small size of the source (vertical dimension < 1 mm) has allowed us to eliminate the first window, which is necessary in a standard diffractometer [1,2]. A second pin-hole F_2 with diameter $\varnothing = 0.7$ mm is located at distance $d = 500$ mm from F_1 in order to cut off the parasitic radiation generated from the edges of F_1 . The use of pin-holes instead of linear windows, motivated by the high intensity and high brightness of the source, does eliminate the usual necessity of desmearing correction for the experimental data [1]. The pin-holes were perforated in thin lead foils, 0.5 mm thick. Lead presents a high absorption coefficient and no emission lines in the X-ray energy range emitted from Adone. They

were machined to a truncated-cone shape with the minor base towards the source in order to eliminate reflections at grazing angle from the incident beam. The lead disks in which the pin-holes were perforated form the bases of a hollow cylinder which can be moved by micrometric screws for optical alignment with the incident radiation. The cylinder is partly inserted in the experimental chamber (where the sample is allocated) by means of vacuum feedthroughs, and is kept at the same pressure, typically 10^{-3} bar (fig. 1). The optical parameters of the collimator are: divergence $2\alpha = 8 \times 10^{-5}$ rad; acceptance angle of the system F_1-F_2 , $2\beta = 2.4 \times 10^{-3}$ rad; sample diameter irradiated by the primary beam $d_1 = 0.54$ mm; detector diameter irradiated by the primary beam $d_2 = 0.58$ mm; detector diameter irradiated by residual parasitic scattering $d_3 = 1.2$ mm. As an example we give also the dimensions of the X-ray beam spot at F_1 , which are 15×3 mm² at 6.0 keV when using a Si-(111) crystal.

We wish to mention that the optical alignment of the apparatus requires a standard procedure that takes account of the fact that the collimation divergency of the diffractometer, 2α , is much smaller than the acceptance angle 2β of the system F_1-F_2 (fig. 2). Therefore, by means of micrometric adjustment of F_2 , the X-ray beam from the monochromator can always be confined within the acceptance angle 2β . For the same reason, there is no problem regarding the stability of the electron beam circulating in the storage ring. Under normal conditions of operation, the stability of the electron beam in Adone is better than $80 \mu\text{m}$, a value much smaller than the transverse beam dimension. Moreover, the effect of the instability on the position of the X-ray beam at F_2 is reduced by the ratio of the distance F_1-F_2 (0.5 m) to the distance F_1 -source (20 m). This stability is very well compatible with the values of 2α and 2β .

3. Experimental chamber

The sample can be placed at a distance of 5 mm from F_2 in an aluminium chamber kept at a pressure of 10^{-3} bar. Solid samples or cells for liquid samples can be moved by micrometric screws for better optical alignment with the incident beam. Either a thermostat operating in the range -50 to $+100^\circ\text{C}$ with 0.01°C precision or a high temperature thermostat for cells with mica windows can be used for liquid samples. The exit window of the chamber is a mylar window of $12 \mu\text{m}$ thickness and 40 mm diameter. We can use four such windows placed perpendicular to the direction of the incident beam in order to collect radiation diffracted also at large angles. One window larger than 40 mm could have not been used because of the mechanical stresses due to the pressure difference at the exit of the chamber.

4. Goniometer

The basic design scheme of the goniometer carrying the detector is shown schematically in fig. 4, and a photograph of it is shown in fig. 5. It can be rotated around the axis of the incident beam and angularly inclined to this axis. The rotation motion is produced by a stepping-motor which transmits the movement to the goniometer by means of a scaler 1:10 and a cog-belt. The angular rotation for one half-step is 0.36° . The motion controlling the inclination to the axis of the incident beam is produced by a stepping-motor which moves a work-driver via a cog-belt. The worm-driver is mounted along a slide and can move a second slide along the first one which remains fixed (fig. 5) (These two slides form the goniometer. The detector can be allocated on the second slide.) The length of the slides is 500 mm, and their maximum translation is 300 mm with a resolution of $5 \mu\text{m}$. The slides have curvilinear shape with a radius of 728 mm. This value of the radius is the best we can obtain by using mechanical machines with numerical control. By means of this arrangement, the combined use of translational and rotational motions allows the detector placed on the goniometer to be moved along the reflection spherical surface with the sample at the centre.

The three-dimensional movements of the goniometer are controlled by a control-module which determines both the preselection of the operational mode of motion and its velocity by the choice of the frequency of the control pulses. The number of these pulses can be read by two counters LABEN mod. 6119 which can also give the exact positions of the detector on the goniometer, by

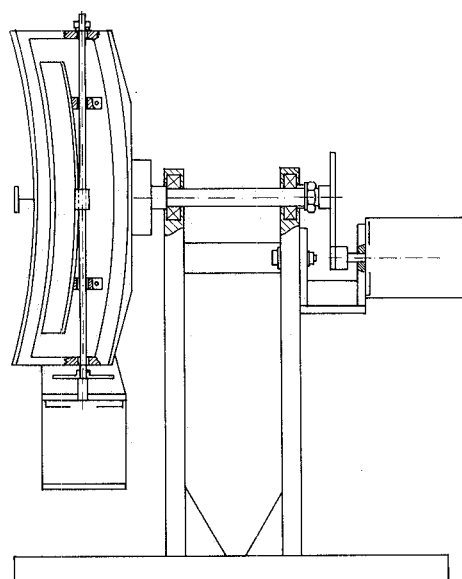


Fig. 4. Basic design scheme of the goniometer.

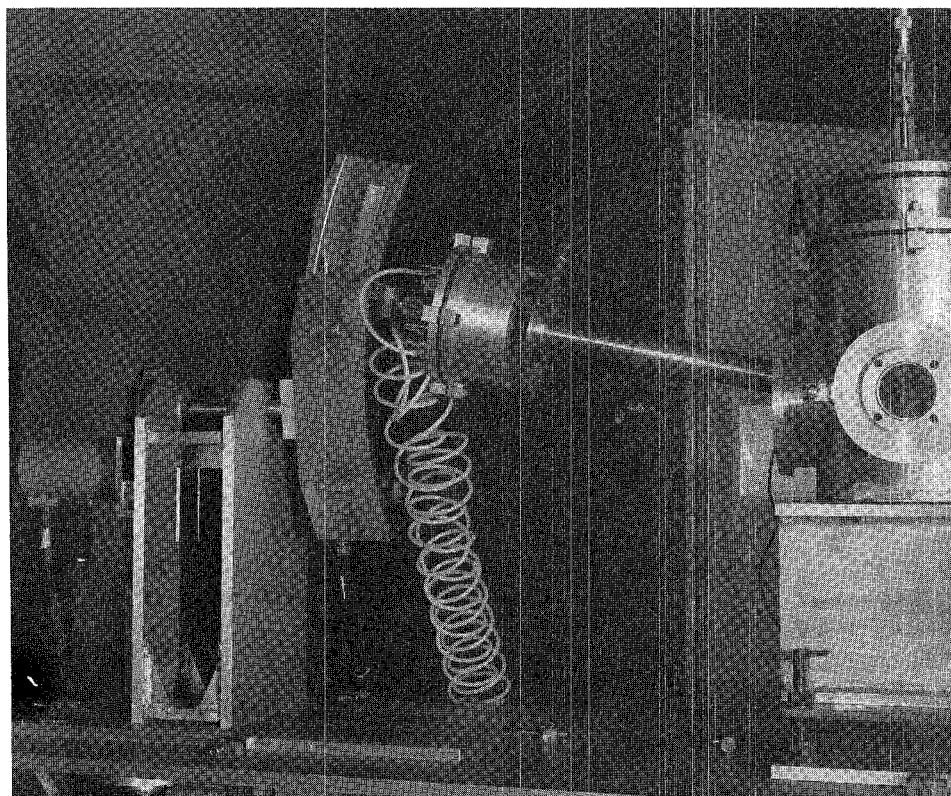


Fig. 5. Photograph of the goniometer slides and detector.

using a timer and printers. The rotation motion can also be controlled by an angular contact-encoder. All the electronics has been installed at a distance of 20 meters from the apparatus for radiation safety reasons around synchrotron radiation facilities.

5. Detector

During recent years, the development of both one-dimensional and two-dimensional X-ray position-sensitive detectors has been most significant in the field of small-angle scattering and diffraction. Very common detectors of this class are the noble gas detectors which have high efficiency and high counting rate capability. The most common one-dimensional detector is a proportional detector which gives the position on the anode-wire of the avalanche electrons produced by the ionizing photon [3]. The measurement of this position is made by using a delay-line behind, and close to, the anode wire. Spatial resolution of the order of 0.5 mm are obtained. The most common two-dimensional position-sensitive detector is the multiwire chamber, formed by a plane of anode wires places between two planes of crossed cathode wires [3]. The avalanche discharge, in-

duced by the ionizing photon mostly at one anode wire, induces signals on a few neighbouring cathode wires (within a range of 6–20 mm) of both planes. The centre of gravity of the amplitudes of the signal on each cathode plane gives the position of the ionizing photons in each corresponding plane with a spatial resolution of ~ 1 mm (fwhm) [3].

More recently, a new position-sensitive detector of the class of gas detectors has been developed by our group, to be used with synchrotron radiation source: the X-ray drift chamber [4,5]. A two-dimensional X-ray drift-chamber was tested at Frascati two years ago [6], and it is now in operation with the diffractometer presented in this paper. A one-dimensional cylindrical drift chamber can also be used when required by particular experiments. In the following, we describe these two detectors, and summarize briefly their mechanisms of operation and properties. (see details in refs. 4 and 6).

5.1. Two-dimensional drift chamber

The scheme of the two-dimensional drift chamber is shown in fig. 6. The chamber has a drift region between grid and field electrode in which the electrons, that are

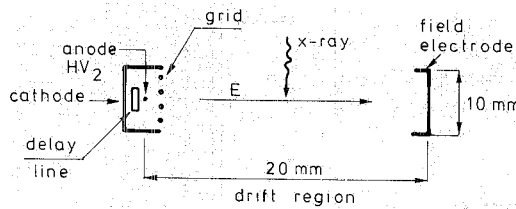


Fig. 6. Scheme of the two-dimensional drift chamber. The length of 20 mm includes the thickness of the cathode-frame.

produced by the incident photon absorbed by the gas mixture (argon 66%, isobutane 30%, methylal 4%) at the time t_0 in the position $P(x, y)$, can travel toward the anode guided by the constant electric field E with constant velocity v . The signal is received at the anode at the time t_1 , when the avalanche of the secondary electrons is produced. The coordinate x of $P(x, y)$ is given by $x = v(t_1 - t_0)$. In general, with a conventional X-ray source we cannot measure the time t_0 because the X-ray photon is totally absorbed by the gas in the chamber. However, when the source is a pulsed synchrotron radiation beam, we can detect a signal at the time t_0 from the radiation flashes emitted by the source. These light flashes are actually emitted with the same time-structure as the electron bunches circulating in the storage ring. Obviously, the position of the photons originating from a given bunch on the detector area can be correctly determined by using the reference time t_0 associated with the same bunch. The maximum drift time $(t_1 - t_0)$ along the whole length of the chamber must then be less than the bunch periodicity. For Adone, in the single mode operation, the electron bunches have a duration time of 1.2 ns and a periodicity of 351 ns. As the drift velocity in our chamber is $50 \mu\text{m}/\text{ns}$, the maximum drift length permitted for an experiment turns out to be 17.5 mm. This is not usually a limitation for small-angle scattering experiments. However, in order to collect radiation scattered at larger angles, as may be the case in diffraction experiments, the detector can be installed on the goniometer described above and can be moved along an arc of 0.35 rad.

The positional coordinate y of the incident photon is obtained by measuring the time difference at the two ends of the delay-line in the signal induced by the anode signal. The delay-line is placed behind, and close to, the anode. The precision of the measured coordinate x is determined by the intrinsic spatial precision of the detector, which in turn is determined by the range of the photoelectrons in the gas. For instance, at 5.0 keV, the photoelectron range is $100 \mu\text{m}$. The spatial resolution in the coordinate y is limited by the range of the avalanche discharge producing the signal on the anode and inducing the signal on the delay-line. This is in our case about $400 \mu\text{m}$.

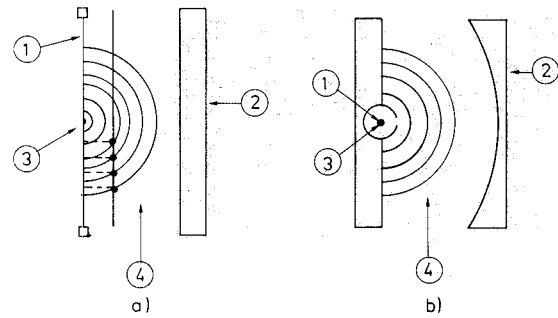


Fig. 7. Some features of the mechanism of operation of the drift chambers: a) two-dimensional drift chamber; b) one-dimensional cylindrical drift chamber. 1 - anode wire; 2 - field electrode; 3 - primary beam of radiation; 4 - drift region.

Both signals, from the anode wire and from the delay-line, can be read by a two-dimensional multichannel-analyzer which displays the cartesian product $x \times y$ on the screen.

5.2. One-dimensional cylindrical drift chamber

The two-dimensional detector described above, if used as a detector for one coordinate (x or y) of the incident photon, presents the following limitation. With reference to fig. 7a, with the primary beam propagating in a direction perpendicular to the anode wire, we notice that the detector is not able to discriminate between two events occurring at different points at the same distance from the anode (for instance, along circles concentric to the anode). In other words, the avalanche discharge produced by such events occur at the same time on the anode wire. On the other hand, scattering experiments on solid or liquid disordered systems give isotropic patterns around the primary beam which can be well measured by using detecting devices with the

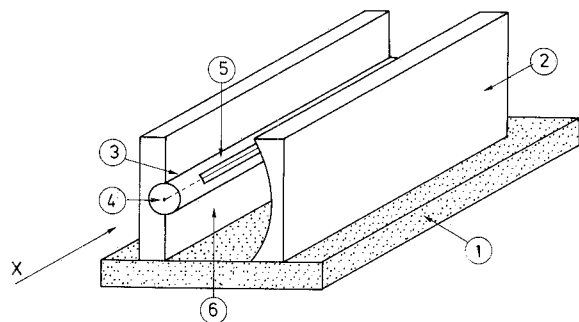


Fig. 8. View of one-dimensional cylindrical drift chamber: 1 - PVC frame; 2 - field electrode; 3 - proportional counter; 4 - anode wire; 5 - electron acceptance window; 6 - drift region.

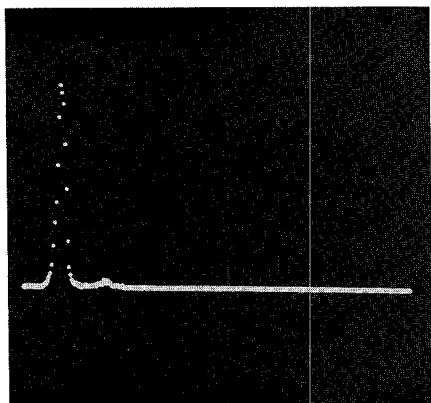


Fig. 9. One-dimensional pattern of a circular window, 0.5 mm diameter, displayed on the multichannel analyzer. Resolution: $30 \mu\text{m}/\text{channel}$. Recording time: 150 s. Photon energy: 11 keV.

same symmetry properties. Therefore, for this class of experiments we have developed the following one-dimensional cylindrical chamber that replaces the two-dimensional detector in the diffractometer, when required. Simply, the chamber has cylindrical symmetry around the anode wire, which is aligned parallel to the incident beam (fig. 7b). The cathode and the field electrode are cylinders concentric to the anode, and a radial drift electric field is thus obtained. A constant drift velocity v is still given to the electrons by working in the saturation region of the argon isobutane-methylal mixture filling the chamber. For details, see for instance ref. 7, par. 3. The anode is made of golden tungsten wire with 2% rhenium, with a diameter of $10 \mu\text{m}$ (fig. 8).

As conclusion to the presentation of our apparatus, as an example we show in figs. 9 and 10 patterns of two windows obtained on the diffractometer by using the X-ray beam at Adone and the above described one-dimensional and two-dimensional detectors.

We are grateful to Mr. Remo Bolli for this collaboration and suggestions for the mechanical parts of the apparatus, to Mr. Massimo Brolatti for the careful design, and to the Staff of the Photographic Shop.

References

- [1] A. Guinier, X-ray Diffraction (W.H. Freeman and Co., London, 1963), Ch. X; A. Guinier and G. Fournet, Small-

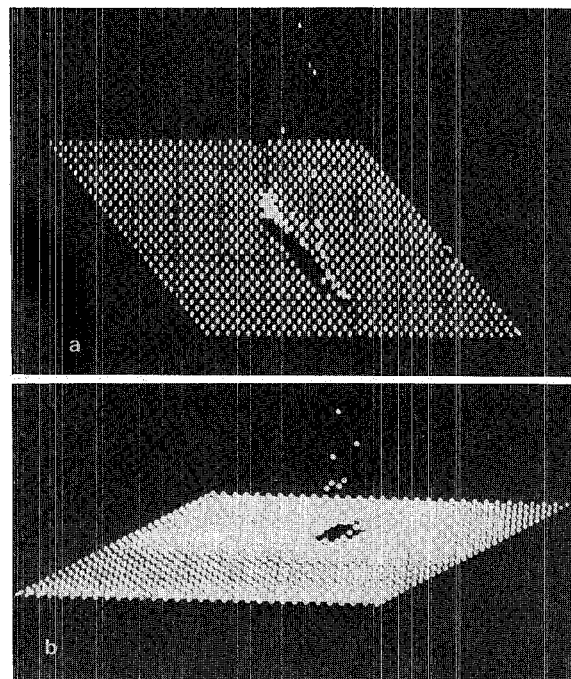


Fig. 10. Two-dimensional patterns of two windows obtained on the diffractometer displayed on the multichannel analyzer in the 4 (32×32) operation mode: a) rectangular window ($0.5 \times 1.5 \text{ mm}^2$); b) circular window ($\varnothing = 0.5 \text{ mm}$). Display points of xy plane represent the intersection of the x and y coordinate (relative channels within a memory group). The points are vertically displayed (z -coordinate) in linear relationship to the digital data stored in each channel. x -direction resolution: $100 \mu\text{m}/\text{channel}$. y -direction resolution: $160 \mu\text{m}/\text{channel}$. Recording time: a) 150 s; b) 100 s. Photon energy: 11 keV.

angle Scattering of X-rays (J. Wiley and Sons, London, 1955). Ch. 3.

- [2] L. Allocca, M. Iannuzzi and A. La Monaca, Frascati Report LNF-82/40 (1982).
 [3] For references, see for instance, J. Schelten and R.W. Hendricks, *J. Appl. Cryst.* 11 (1978) 297.
 [4] M. Iannuzzi and A. La Monaca, *Japan. J. Appl. Phys., Supplement 17-2* (1978) 469.
 [5] A. La Monaca, Frascati Report LNF-79/59 (1979).
 [6] M. Iannuzzi and A. La Monaca, *Nucl. Instr. and Meth.* 201 (1982) 197.
 [7] A. Breskin, G. Charpak, B. Gabioud, F. Sauli, N. Traunter, W. Duinker and G. Schultz, *Nucl. Instr. and Meth.* 119 (1974) 9.